

Geology of the Decar area north of Trembleur Lake, NTS 93K/14



Dejan Milidragovic^{1, a}, Ryan Grundy^{1, 2}, and Paul Schiarizza¹

¹British Columbia Geological Survey, Ministry of Energy, Mines and Petroleum Resources, Victoria, BC, V8W 9N3

²School of Earth and Ocean Sciences, University of Victoria, Victoria, BC, V8W 3P6

^acorresponding author: Dejan.Milidragovic@gov.bc.ca

Recommended citation: Milidragovic, D., Grundy, R., and Schiarizza, P., 2018. Geology of the Decar area north of Trembleur Lake, NTS 93K/14. In: Geological Fieldwork 2017, British Columbia Ministry of Energy, Mines and Petroleum Resources, British Columbia Geological Survey Paper 2018-1, pp. 129-142.

Abstract

Upper Paleozoic to Lower Jurassic deformed rocks of the Cache Creek terrane in the Decar area, central British Columbia, include partly to completely serpentinized or carbonate-altered mantle tectonite (Trembleur ultramafite), flanked on both sides by predominantly argillaceous and siliceous fine-grained sedimentary rocks and aphanitic mafic volcanic rocks of the Sowchea succession and Sitlika assemblage. The volcano-sedimentary units have been metamorphosed at greenschist-facies as evidenced by actinolite-chlorite-epidote mineral assemblages in the metabasalts. Minor wacke, marble, and conglomerate are interbedded with the fine-grained metasedimentary rocks. The highest metamorphic grade (amphibolite facies) in the area are in the Rubyrock igneous complex, a Late Permian predominantly gabbro-dioritic intrusive complex that may represent the crustal portion of a dismembered ophiolitic sequence, formed above the harzburgite and lesser dunite of the Trembleur ultramafite. The entire Decar area displays a strong, relatively uniform, steeply dipping, northwest-striking structural fabric that may reflect regional northeast-southwest directed shortening during the collision of the Cache Creek terrane with Stikinia.

Keywords: Cache Creek terrane, Decar, awaruite, Trembleur, ultramafite, ophiolite

1. Introduction

The Cache Creek terrane of the North American Cordillera (Fig. 1) is a belt of tectonically imbricated Paleozoic and Mesozoic oceanic rocks, including volcanic and volcanoclastic rocks, chert, argillite, carbonate, conglomerate, and wacke, and ultramafic mantle tectonite with associated mafic plutonic rocks (Monger, 1977; English and Johnston, 2005; Nelson et al., 2013). Recently, Britten (2017) reported coarse-grained (>200 μm) awaruite (Ni_3Fe) mineralization of potential economic significance in Cache Creek ultramafic rocks on the Decar property, approximately 90 km northwest of Fort St. James in central British Columbia. Finer grained awaruite mineralization is also associated with ultramafic rocks of the northern Cache Creek terrane (Britten, 2017). Awaruite is ubiquitous in serpentinized ultramafic rocks (e.g., Nickel, 1956; Chamberlain et al., 1965; Ahmed and Bevan, 1981; Beard and Hopkinson, 2000; Klein and Bach, 2009) and the physicochemical conditions that lead to its early development are relatively well known (Frost, 1985; Sleep et al., 2004; Frost and Beard, 2007; Foustoukos et al., 2015). However, coarse-grained (>200 μm) mineralization is relatively uncommon (e.g., Sciortino et al., 2015; Britten, 2017), and how economically viable, coarse-grained awaruite deposits form is poorly understood.

Rocks of the Cache Creek terrane are widely regarded as a tectonically juxtaposed mix of: 1) oceanic lithosphere from varied and disparate paleoenvironments; and 2) subduction-

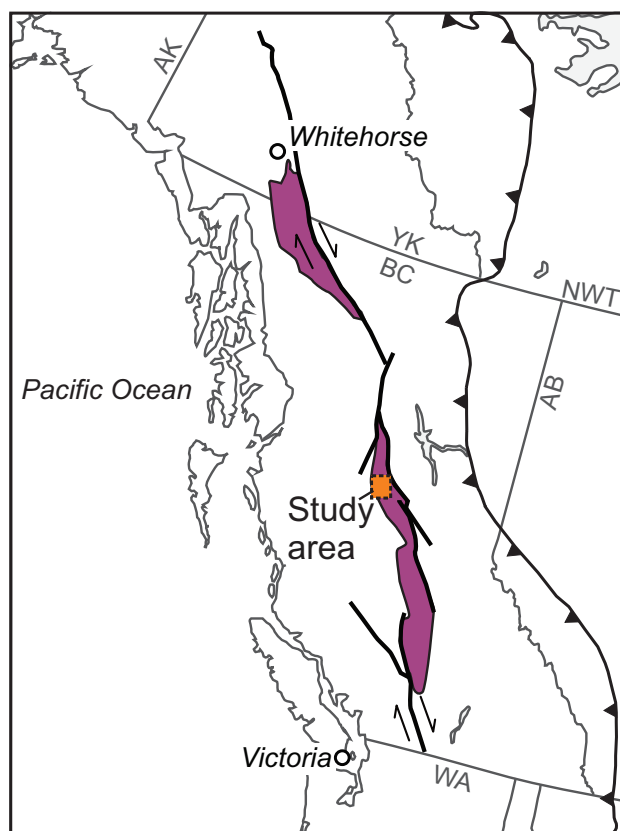


Fig. 1. Location of the study area and distribution of Cache Creek terrane (purple) in the Canadian Cordillera.

related volcanic and sedimentary rocks deposited in a forearc setting (Mihalynuk et al., 1994; Struik et al., 2001; English and Johnston, 2005; English et al., 2010). However recently, McGoldrick et al. (2017) suggested that original stratigraphic relationships in Cache Creek rocks of northwestern British Columbia are preserved, and argued for a genetic link between mantle tectonite and overlying arc basalts, placing them in a supra-subduction zone tectonic setting that is distinct from the intraoceanic setting indicated by ocean island basalt (OIB)-type volcanic rocks intercalated with thick carbonate successions. Accordingly, the Cache Creek terrane in northwestern British Columbia may consist of two fundamentally different and mappable domains: 1) intraoceanic carbonate and intraplate volcanic rocks and 2) an upper plate assemblage of arc mantle lithosphere, mafic and ultramafic cumulates, and related volcanic and sedimentary rocks (ophiolite).

At present, understanding of the stratigraphy and tectonic evolution of the Cache Creek terrane in central and southern British Columbia lags behind that of the Cache Creek terrane in northwestern British Columbia and Yukon. Thus, we undertook a 1:50,000 mapping and sampling project in the area of the Decar occurrence (part of Trembleur Lake, NTS 93K/14) to update existing geological maps, understand the petrological evolution of the mantle tectonite that hosts the prospective awaruite mineralization, and develop a chemostratigraphic framework for the Permo-Triassic volcanic and related intrusive rocks. Herein, we describe the preliminary results of this mapping and provide petrographic descriptions of the principal rock types.

2. Geological setting

The Cache Creek terrane is a ~1500 km-long belt of oceanic rocks exposed along the central axis of British Columbia (Fig. 1; Monger, 1977; Nelson et al., 2013). It records deposition of vast carbonate platforms, lesser ribbon chert, argillite, and coarse siliciclastic rocks, build-up of basaltic oceanic plateaus and seamounts, and emplacement of mafic to intermediate intrusive rocks (Monger, 1975; Mihalynuk et al., 1999; Struik et al., 2001; English et al., 2010). This activity is temporally bracketed by the Upper Mississippian foraminifera of the Kedahda Formation near Atlin (Monger, 1975) and the Middle Jurassic collision of the Cache Creek terrane with Stikinia (ca. 172 Ma), as defined by the oldest postkinematic intrusions in the Cache Creek terrane (Mihalynuk et al., 2004). Paleozoic to Middle Triassic macrofossils and microfossils with Tethyan affinities indicate that the Cache Creek terrane was in the Panthalassan Ocean, far from the North American continent, during most of its ≥ 160 m.y. existence (Monger and Ross, 1971; Orchard et al., 2001). A key feature of the Cache Creek terrane is the widespread occurrence of ultramafic rocks (Tardy et al., 2001; Lapierre et al., 2003; English et al., 2010; McGoldrick et al., 2016), interpreted to have originated as lithospheric mantle beneath the Cache Creek ocean that was emplaced as tectonic slivers.

The current tectonostratigraphic framework for Cache Creek

terrane in central British Columbia is based on 1:100,000-scale mapping by the Geological Survey of Canada and the British Columbia Geological Survey between 1995 and 2000 (MacIntyre and Schiarizza, 1999; Schiarizza and MacIntyre, 1999; Struik et al., 2001, 2007). The terrane includes three structurally disrupted components: 1) the Cache Creek complex 2) the Sitlika assemblage, which is typically found structurally beneath ophiolitic rocks of the Cache Creek complex in the western part of the terrane, and includes a Permo-Triassic intra-oceanic arc complex and an unconformably overlying Late Triassic-Early Jurassic siliciclastic succession; and 3) the Tezzeron succession, a Late Triassic-Early Jurassic siliciclastic unit along the eastern edge of the terrane, adjacent to the Quesnel arc terrane.

The Cache Creek complex, forming most of the Cache Creek terrane in central British Columbia, is subdivided into numerous subunits, commonly juxtaposed across Early to Middle Jurassic thrust faults and/or younger structures (Struik et al., 2001). The central and eastern parts of the complex consist mainly of rocks that probably accumulated as an accretionary complex (Struik et al., 2001). This part of the complex includes the Sowchea succession, consisting of Pennsylvanian-Early Jurassic fine-grained siliceous sedimentary rocks (cherty argillite and slate to muddy chert), with lesser limestone, greywacke, basalt, andesite, and conglomerate containing intraformational siltstone clasts. It also includes several carbonate rock-rich units, including: Pennsylvanian-Early Permian carbonate rocks with local thin basaltic breccia, volcanoclastic rocks, and ribbon chert (Pope succession); Middle-Late Permian micritic and bioclastic limestone (Copley succession); and Permian-Triassic limestone, limestone breccia, shale, and basaltic tuff (Kloch Lake succession). Other subunits of the Cache Creek Complex, found mainly to the west, are interpreted as components of a dismembered ophiolite (e.g., Boudier and Nicolas, 1985). These include: 1) harzburgite and lesser dunite, pyroxenite, and peridotite (Trembleur ultramafite), which display variable amounts of serpentinization, and calc-silicate alteration; 2) greenschist-facies mafic to ultramafic, altered and variably deformed intrusive and volcanic rocks assigned to the Rubyrock igneous complex; and 3) basalt and chert units, locally cut by mafic dikes and sills, that are spatially associated with the Trembleur ultramafite (North Arm succession of Schiarizza and MacIntyre, 1999, and MacIntyre and Schiarizza, 1999).

3. Geology of the Decar area

Our mapping in the Decar area (Fig. 2) reveals that the central part is underlain by ophiolitic rocks of the Cache Creek complex, including the Trembleur ultramafite and the Rubyrock igneous complex. To the southwest are siliciclastic rocks that belong to the upper part of the Sitlika assemblage (Upper Triassic-Lower Jurassic; MacIntyre and Schiarizza, 1999; Schiarizza and MacIntyre, 1999). Following Struik et al. (2001) we assign a basalt-chert unit, flanking the ultramafic rocks to the northeast, to the Sowchea succession. This unit was included in the North Arm succession (of suspected ophiolite affinity) by Schiarizza

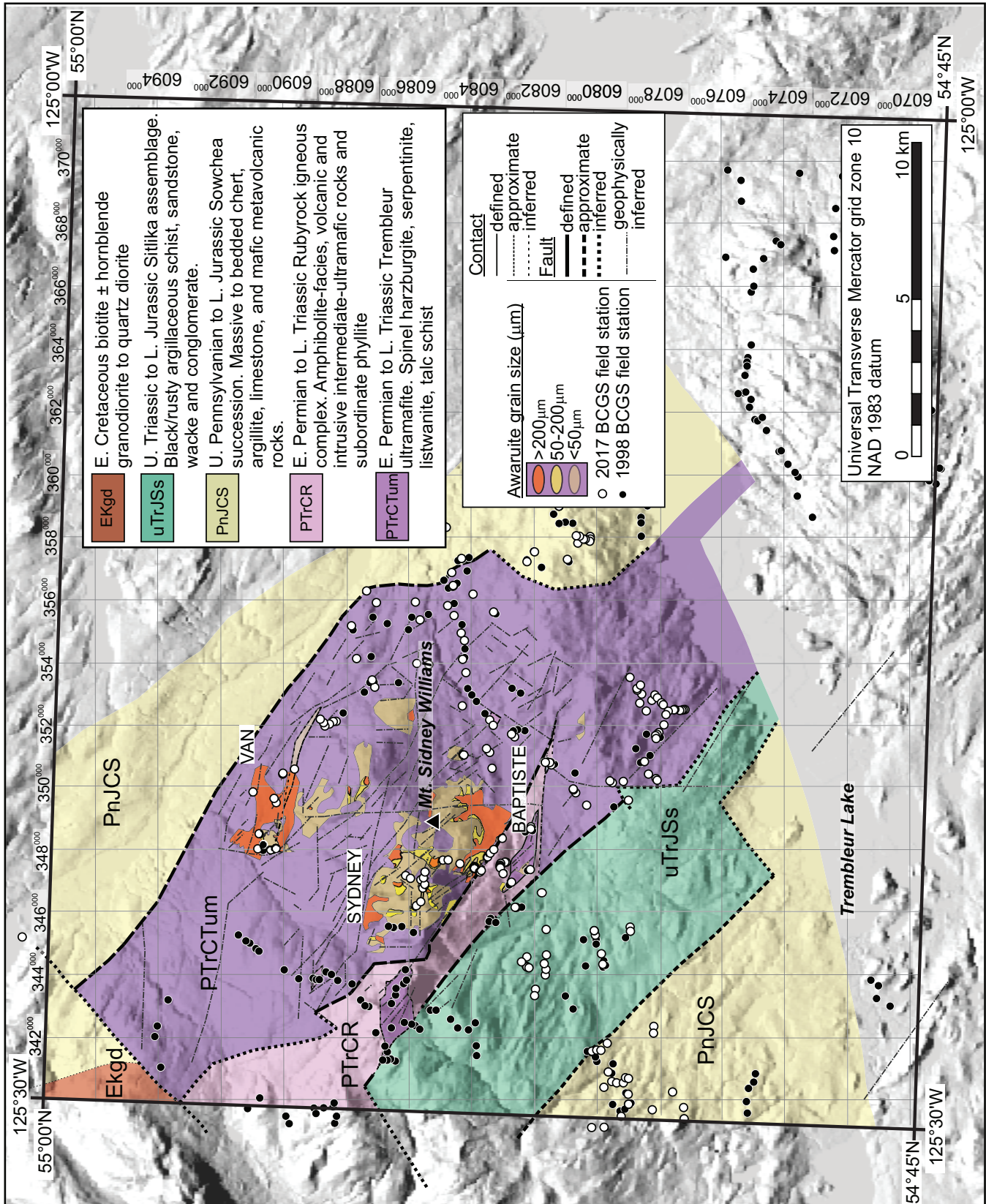


Fig. 2. Preliminary geology of the Decar area north of Trembleur Lake (93K/14).

and MacIntyre (1999) and MacIntyre and Schiarizza (1999). We also mapped a sedimentary-volcanic succession adjacent to the Sitlika assemblage in the southwestern part of the study as Sowchea succession because it is very similar to rocks exposed to the northeast. Previously, these rocks, specifically a unit of mafic sills and dikes with abundant screens of basalt and chert that was interpreted as transitional between the predominantly intrusive Rubyrock complex and the predominantly supracrustal North Arm succession (Schiarizza and MacIntyre, 1999; MacIntyre and Schiarizza, 1999), were included in the Rubyrock igneous complex. Although the contact between the Sitlika assemblage and the Sowchea succession is not exposed, it is interpreted to be structural. The structural juxtaposition of the two units is supported by the increase in the relative intensity of deformation near the contact, and the sharp transition from rocks with relatively high magnetic signatures to the southwest to rocks with relatively low magnetic signatures to the northeast, which follows the regional structural fabric (Struik et al., 2007) and coincides with the inferred fault contact.

Peridotite of the Trembleur ultramafite is weakly to strongly altered to either serpentinite or listwanite (magnesite \pm serpentine \pm calc \pm quartz; Hansen et al., 2005). Locally, serpentinitized peridotite hosts significant coarse-grained (50-400 mm) awaruite (Ni_3Fe), which Britten (2017) attributed to relatively late, fracture- or shear zone-focused, high-temperature ($\geq 400^\circ\text{C}$) serpentinitization (antigorite-lizardite) accompanied by growth of metamorphic olivine after Cache Creek terrane accreted to North America.

The Rubyrock igneous complex is structurally interleaved with the western part of the Trembleur ultramafite and is widely regarded (Schiarizza and MacIntyre, 1999; Struik et al., 2001; Britten, 2017) as the crustal portion of the ophiolite. The only age from the complex is 257 ± 5 Ma, obtained from a tonalite lens (unpublished TIMS U-Pb zircon date; Struik et al., 2001; Struik et al., 2007).

4. Main rock types

4.1. Trembleur ultramafite

4.1.1. Peridotite

Weakly serpentinitized peridotite is exposed in moderately to sparsely vegetated, elevated regions on Mount Sydney Williams and the unnamed ridge to the northeast (Fig. 2). The peridotite weathers yellow-brown to grey (Figs. 3a-b), and is dark grey to black on fresh surface. The dark fresh surface and weak to moderate magnetic susceptibility of the peridotite reflect microscopic secondary magnetite formed during serpentinitization. Warty textured, medium- to coarse-grained massive harzburgite, containing trace amounts of clear clinopyroxene ($\sim 1\%$) and medium brown spinel ($\leq 2\%$), is the most common peridotite lithology. Individual olivine crystals are generally not discernible in hand sample, whereas orthopyroxene crystals exhibit strong cleavage and light grey alteration (bastite), which ranges from a thin surficial coating to nearly complete replacement in highly serpentinitized harzburgite. In thin section, olivine crystals are ≤ 3 mm across,

display kink banding and/or undulose extinction, and have curvilinear grain boundaries. Orthopyroxene porphyroclasts are typically coarser (≤ 5 mm) and more euhedral than olivine. Exsolution of clinopyroxene along orthopyroxene cleavage planes is common and some grains display deformation of the exsolution lamellae. Orthopyroxene grains that are nearly completely bastite-altered usually have rims of black secondary spinel that increase in width with increasing degrees of serpentinitization. Clinopyroxene is not discernible in hand sample, but is distinguished from orthopyroxene in thin section by smaller grain size and cleavage-parallel exsolution of ubiquitous, thin, closely-spaced (< 10 mm) laminae of secondary spinel (Figs. 3c-e). Primary spinel is characteristically irregular, with a vermicular, interstitial habit (Fig. 3f), and commonly displays holly-leaf texture within orthopyroxene porphyroclasts. Primary spinels in the least serpentinitized samples are medium brown to dark red and, with increasing degrees of serpentinitization become black along grain boundaries, likely from magnetite alteration. Sulphide occurs in trace quantities as very small (< 10 mm) subhedral crystals. Harzburgite typically has a massive appearance (protogranular according to the classification of Mercier and Nicolas, 1975), but locally displays layers of coarser or modally more abundant orthopyroxene. Smooth weathering pods and dikes of replacive dunite (Kelemen and Dick, 1995) are relatively uncommon and are typically in sharp contact with their harzburgite host (Fig. 3b). Rare, thin (< 5 cm) dikes of coarse-grained pyroxenite, which locally cut harzburgite, are discordant, and have variable orientation.

4.1.2. Serpentinite

Pervasively ($> 90\%$) serpentinitized peridotite is ubiquitous in the Trembleur ultramafite, forming large homogeneous outcrops, crosscutting less serpentinitized harzburgite, or forming knockers within bodies of listwanite (Figs. 4a-c; 5a). Serpentinite weathers grey-brown, through grey, to light green and typically displays a moderate to strong schistosity, although it may also appear massive. Earliest serpentinitization is marked by growth of lizardite, indicated by hour-glass and mesh textures (e.g., Evans et al., 2013) in the least serpentinitized peridotites, and magnetite. The hour-glass and mesh textures are not evident in more completely serpentinitized peridotites, which feature fibrous to tabular interlocking serpentine, interpreted to be antigorite. Growth of high-relief, fine-grained, metamorphic olivine along serpentine microveinlets is interpreted as the latest and highest temperature alteration of the Trembleur ultramafite. Sample DMI17-10-1 (Figs. 4d-f), collected from the Baptiste deposit (Fig. 2), displays a texture in which the convergence of chrysotile veinlets, lined with olivine, defines 'cores' of antigorite that are mantled by metamorphic olivine. In addition to texture, metamorphic olivine is distinguished from primary mantle olivine by its dark to cloudy appearance in plane-polarized light, and its fine grain size. Identification of metamorphic olivine in Trembleur serpentinite, confirms its previous recognition by Britten (2017). Although awaruite

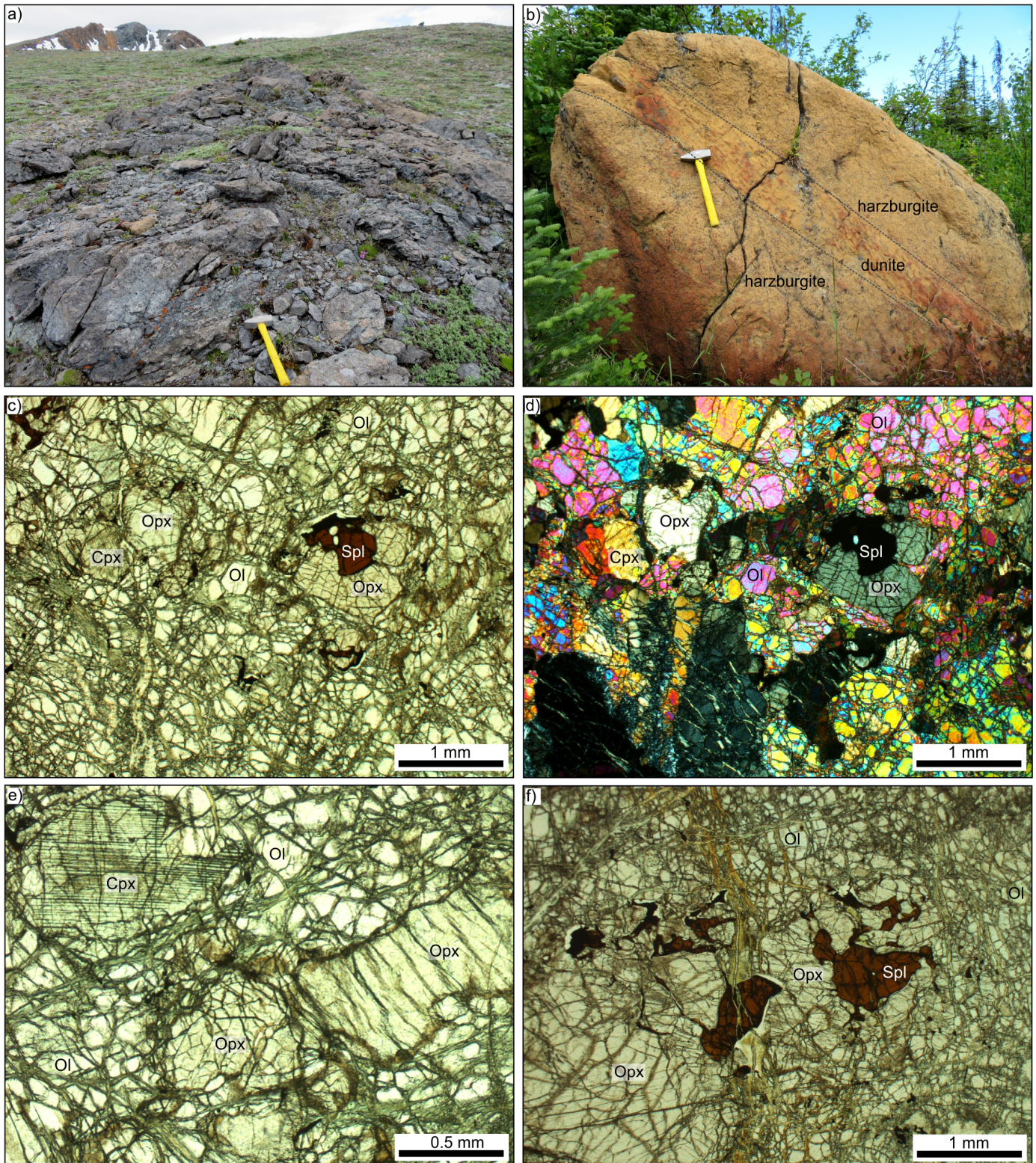


Fig. 3. **a)** An outcrop of harzburgite on the southeast-facing flank of Mount Sidney Williams. The heavily diked central peak is in the background. **b)** A large boulder of yellow-brown weathering harzburgite cut by a ~20 cm wide, smooth-weathering, tabular dunite dike. **c)** Plane-polarized light image of harzburgite 98PSC-33-5 collected from the westernmost peak of Mount Sidney Williams. **d)** Cross-polarized light image of harzburgite 98PSC-33-5. **e)** Plane-polarized light image of a clinopyroxene crystal with thin lamellae of oxide mineral(s) exsolved along cleavage planes. **f)** Plane-polarized light image of irregular, vermicular, spinel crystals intergrown with orthopyroxene. Abbreviations: Ol-olivine, Opx-orthopyroxene, Cpx-clinopyroxene, Spl-spinel.

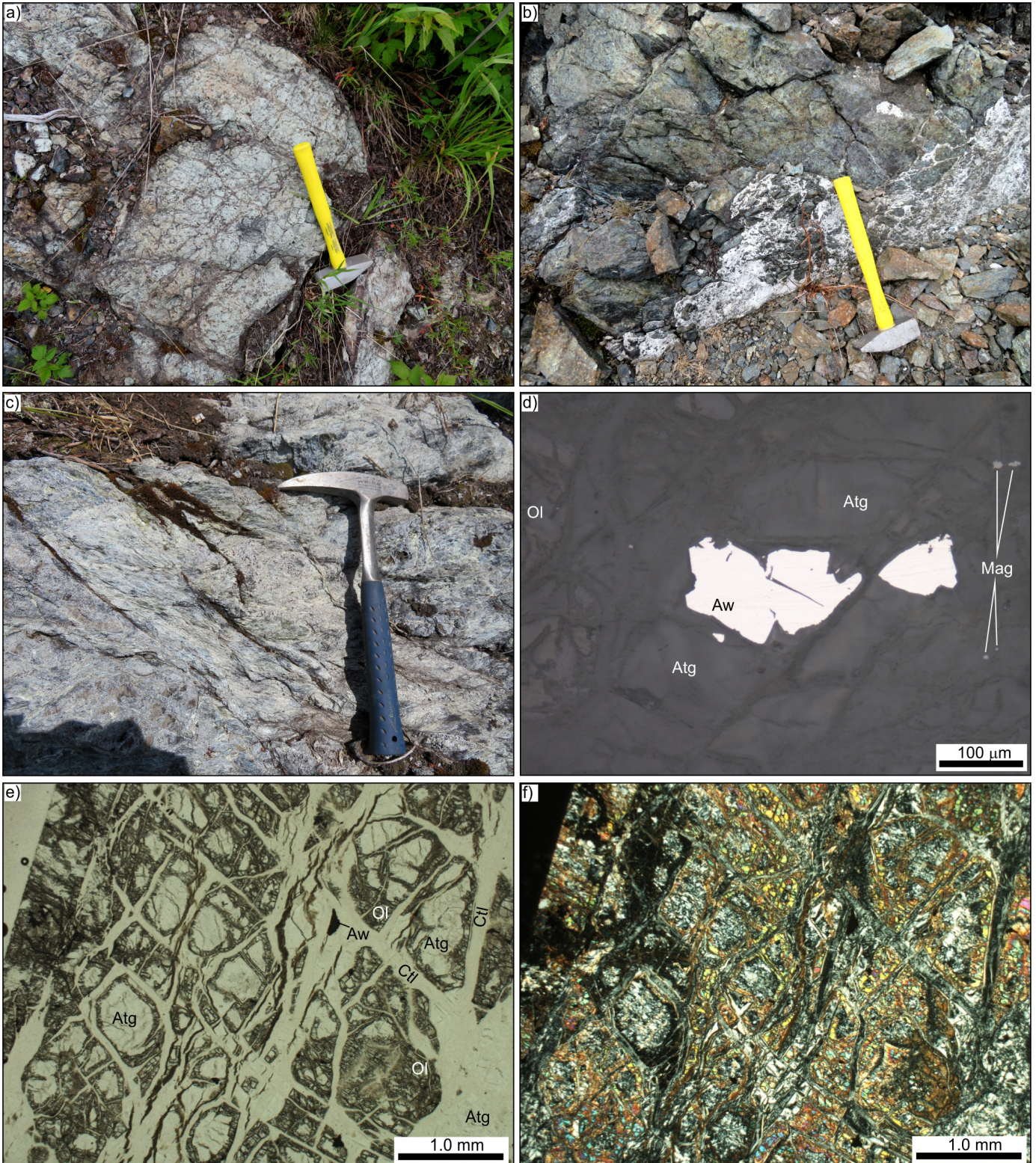


Fig. 4. a) An outcrop of light grey-weathering, homogeneous, serpentinite. b) Dark grey-green-weathering serpentinite cut by a white-weathering breccia. c) Strongly schistose, light grey- to green-weathering serpentinite. d) Reflected light image of anhedral awaruite (Aw) surrounded by antigorite. Higher relief grains on the left side of the image are olivine. e) Plane-polarized light image of sample DMI17-10-1 showing metamorphic olivine growing along microveinlets of serpentinite (antigorite and/or chrysotile) converging to form 'rims' around antigorite. f) Cross-polarized light image of the same sample DMI17-10-1 (same field of view as e). Abbreviations: Atg-antigorite, Mag-magnetite, Aw-awaruite, Ctl-chrysotile, Ol-olivine.

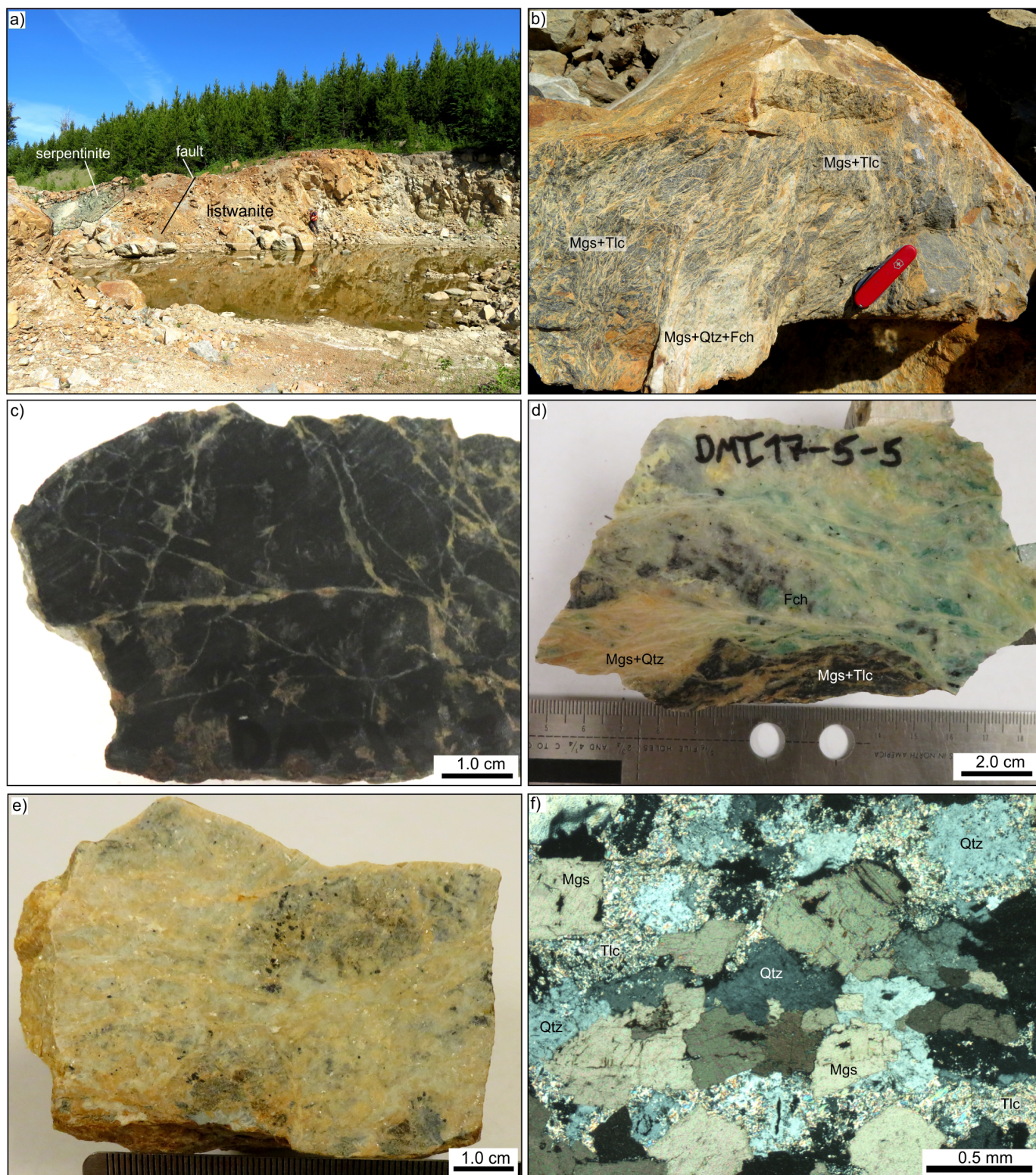


Fig. 5. **a)** Pit exposing mainly rusty-weathering listwanite; also m-scale knockers of green-weathering serpentinite. **b)** Heterogeneous listwanite comprising a dark heavily veined (Mgs+Tlc) domain and a more massive, lighter coloured (Mgs+Qtz+Fch) domain. Magnesite veins in the Mgs+Tlc domain show no preferred alignment. **c)** Hand sample of dark listwanite consisting of magnesite veins, serpentine and talc. **d)** Heterogeneous listwanite with dark domains of Mgs+Tlc and lighter domains of Mgs+Qtz. The conspicuous green colour is due to fine grained fuchsite. **e)** Heavily carbonitized listwanite largely composed of magnesite and quartz. Dark domains may contain relict talc. The dark, euhedral, fine-grained mineral is specular hematite. **f)** Cross-polarized light image of listwanite sample 98PSC-16-6 showing the incomplete carbonation of talc through reaction $Mg_3Si_4O_{10}(OH)_2 + 3CO_2 = 3MgCO_3 + 4SiO_2 + H_2O$ (Hansen et al., 2005). Abbreviations: Mgs-magnesite, Qtz-quartz, Tlc-talc, Fch-fuchsite.

likely formed from the onset of serpentinization (Frost and Beard, 2007; Klein and Bach, 2009), grains sufficiently large for field identification (>100-200 mm) only occur in samples containing antigorite +/-olivine.

4.1.3. Listwanite

Ultramafic rocks in the southeastern and eastern portion of the Trembleur ultramafite (Fig. 2) are extensively CO₂ altered. We apply the term 'listwanite' to all such rocks, following the definition of Hansen et al. (2005). Listwanite is characterized by ubiquitous magnesite, relatively low magnetic susceptibility, and rusty orange-weathering (Fig. 5a). The rusty orange-weathering likely reflects the presence of an ankeritic component in the magnesite, as suggested by Schiarizza and MacIntyre (1999). Significant variations in colour, texture, and hardness occur on hand-sample scale (Figs. 5b-c), reflecting different mineral assemblages including: serpentine-magnesite, talc-magnesite, and quartz-magnesite end members (Figs. 5b-f). High-standing knobs and ridges in the southeastern part of the Trembleur ultramafite are predominantly composed of magnesite and quartz-rich listwanite, hardened by extensive carbonation of serpentine, brucite, and talc. Listwanite also contains minor relict magnetite and may also contain fine-grained, disseminated, emerald green fuchsite, found exclusively with quartz±pyrite±specular hematite.

4.2. Intrusive rocks

Mafic to intermediate intrusive rocks form a major component of the Rubyrock igneous complex, southwest of the Trembleur ultramafite, and occur as small plugs and dikes which intrude and crosscut the ophiolitic and volcano-sedimentary units in the study area. The metaintrusive rocks of the Rubyrock igneous complex (Figs. 6a and b) are interleaved with probable metavolcanic and minor metasedimentary rocks (see section 4.3.2.) and separated from pervasively serpentinized, coarse awaruite-bearing (Baptiste deposit) rocks of the Trembleur ultramafite by a northwest-striking fault. The fault is also marked by a sharp contrast in total field magnetic response between the highly magnetic rocks of the Trembleur ultramafite, and the less magnetic rocks of the Rubyrock igneous complex (Verley, 2011).

Before amphibolite-facies metamorphism, the intrusive rocks of the Rubyrock intrusive suite were predominantly gabbro and diorite, with lesser clinopyroxenite±hornblendite. On the west side of Mount Sidney Williams (Fig. 2), they typically display a strong fabric (Fig. 6a), defined by aligned amphibole and cm- to dm-scale plagioclase-rich and amphibole-poor layers and lenses (Fig. 6b). Accessory titanite and clinozoisite are important metamorphic phases of the Rubyrock intrusive suite.

Homogeneous mafic to felsic intrusive rocks that have not undergone significant metamorphism outcrop throughout the study area and include fine-grained diabase dikes, isolated gabbroic plugs (Fig. 6c), and small felsic bodies with abundant rusty ankerite patches. The relationship between these bodies is uncertain, but they crosscut the ultramafic and volcano-

sedimentary units. An Early Cretaceous granodiorite pluton outcrops in the northwest corner of the study area (Struik et al., 2007), but was not sampled.

4.3. Layered rocks

4.3.1. Metavolcanic rocks

Volcanic rocks, of predominantly basaltic composition are prominent components of the Sowchea succession in both the eastern and western parts of the study area, and of the Rubyrock igneous complex (Fig. 2). They occur as both aphanitic volcanic flows and breccias, locally interbedded with lenses of metasedimentary rock. Primary mineralogy of the volcanic rocks has been extensively obliterated by greenschist facies metamorphism, resulting in light grey to green, weakly to strongly schistose, locally pyritiferous, actinolite-chlorite-epidote rocks (Figs. 7a and b). Amygdules and irregular veinlets, occupied by carbonate, chlorite and/or epidote, are typically the only macroscopic features of the aphanitic rocks (Fig. 7c). Rarely, aphanitic basalts contain plagioclase phenocrysts (Fig. 7d); clinopyroxene phenocrysts have not been observed. Fragmental volcanic rocks are common in both units (Figs. 7e and f).

Volcanic rocks observed in the study area do not display significant petrographic and textural differences. However, English et al. (2010) and McGoldrick et al. (2017) have demonstrated that the geochemical variability of volcanic rocks of the northern Cache Creek terrane may be used for petrological classification, and gaining new insights into the tectono-magmatic evolution of the Cache Creek terrane. These studies identified calcalkaline basalts and island arc tholeiites (IAT), in addition to basalts that span the MORB-OIB (mid-ocean ridge basalt-ocean island basalt) array (Pearce, 2008), adding new complexity to the geodynamic interpretations of the Cache Creek terrane. The relatively few geochemical analyses from the Cache Creek terrane in central British Columbia (Tardy et al., 2001; Lapierre et al., 2003), display a similar degree of variability (McGoldrick et al., 2017), suggesting that, despite the metamorphic overprint and similarities in field appearance, geochemical discrimination is an effective tool for assigning metavolcanic rocks in the study area to lithostratigraphic units. Geochemical analyses of 17 volcanic samples from the study area are ongoing.

4.3.2. Metasedimentary rocks

Metasedimentary rocks occur in the Sowchea succession and the Sitlika assemblage. Both units comprise predominantly fine-grained sedimentary rocks with moderately to well-developed cleavage. The field criteria used to distinguish the two units are the higher relative chert content of the Sowchea metasedimentary rocks versus the more argillaceous nature of the Sitlika assemblage metasedimentary rocks, and the high relative abundance of mafic metavolcanic rocks in the Sowchea succession. In addition, phyllite, chert, and highly fissile siltstone (Fig. 8f) are interlayered as possible rafts/enclaves with mafic metavolcanic and/or metaintrusive rocks

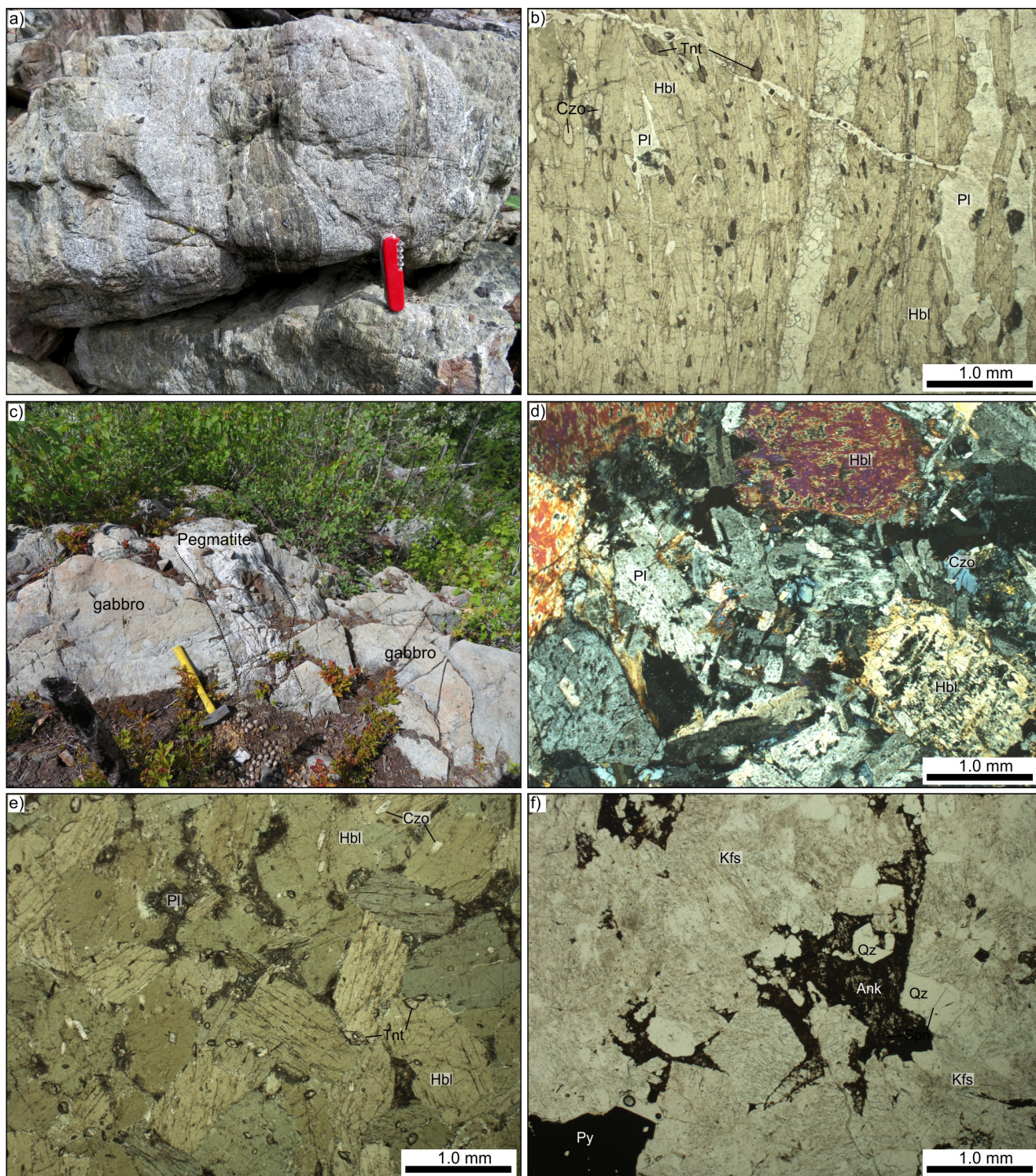


Fig. 6. **a)** Strong fabric in amphibolite-facies metamorphosed intrusive rocks of the Rubyrock igneous complex. Discontinuous lenses of amphibolite are hosted by predominantly plagioclase-rich metagabbro and metadiorite. **b)** Plane-polarized light image of sample 98PSC-14-10-1 collected from a). Strong metamorphic fabric is defined by aligned hornblende crystals and segregations of hornblende and plagioclase. Titanite and clinozoisite are important accessory phases. **c)** Massive gabbro cutting the Sowchea succession, east of Trembleur ultramafite cut by pegmatite. **d)** Cross-polarized light image of a sample DMI17-15-7, from gabbro in c). Clinopyroxene has been pervasively replaced by hornblende, plagioclase is partly saussuritized, and metamorphic clinozoisite is ubiquitous. **e)** Plane-polarized light image of isotropic amphibolite 98PSC-33-91 of the Rubyrock igneous complex, containing interstitial saussuritized plagioclase and accessory clinozoisite and titanite. **f)** Plane-polarized light image of massive quartz syenite DMI17-15-3, which intrudes the Trembleur ultramafite near its eastern contact with the Sowchea succession. The rock is rich (~20%) in rusty weathering carbonate (ankerite) and contains ~3 mm crystals of euhedral pyrite. Abbreviations: Hbl-hornblende, Pl-plagioclase, Czo-clinozoisite, Tnt-titanite, Kfs-K-feldspar, Ank-ankerite.

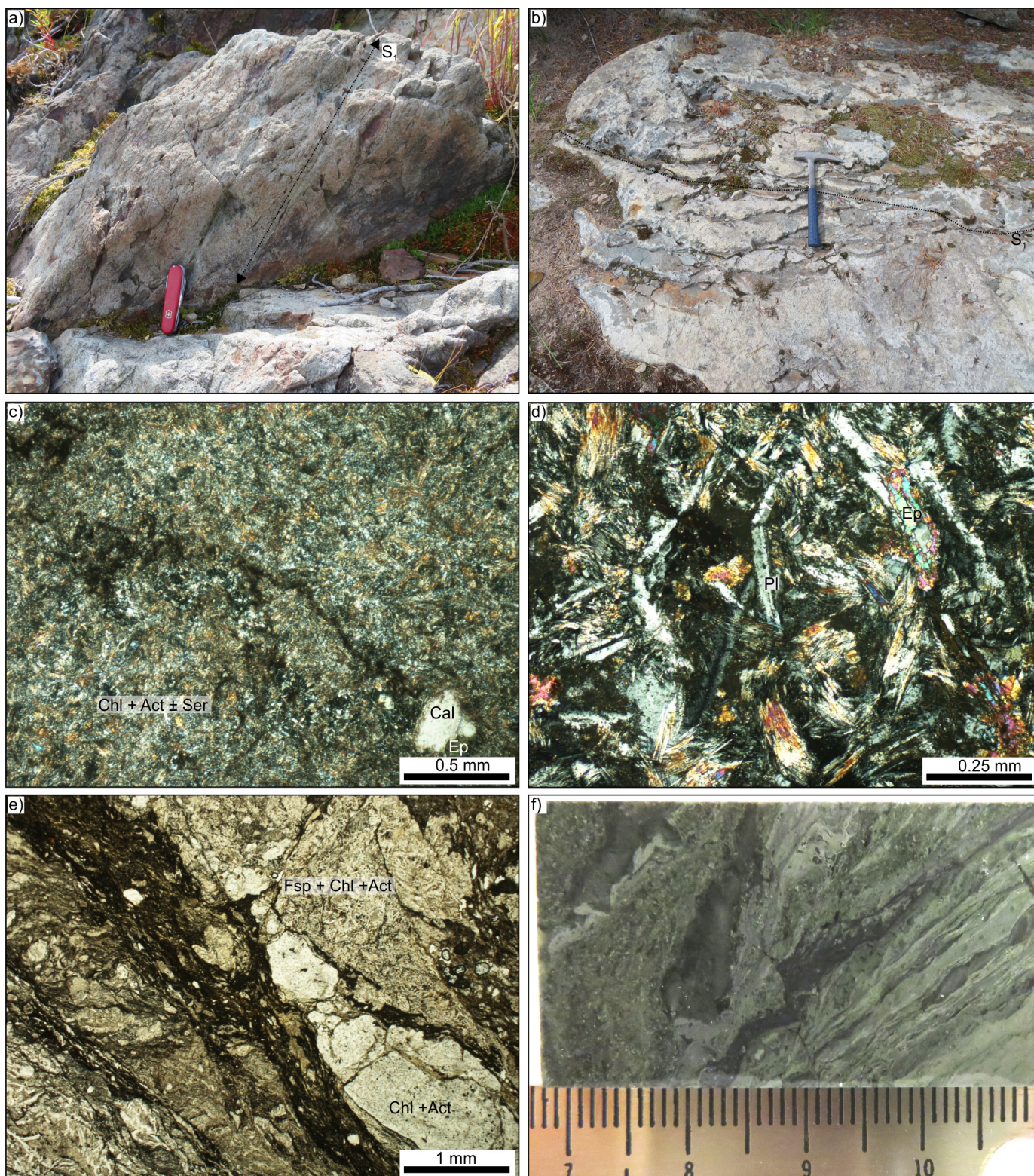


Fig. 7. **a)** Cream-weathering, moderately schistose (S_1), chloritic metabasalt. **b)** Pink-cream-weathering, schistose (S_1) aphanitic metabasalt. **c)** Cross-polarized light image of amygduloidal (calcite+epidote), aphanitic metabasalt (DMI17-1-2). Primary mineralogy has been largely replaced with fine intergrowths of actinolite, chlorite±sericite. **d)** Cross-polarized light image of plagioclase-phyric, aphanitic metabasalt (DMI17-2-15). Groundmass has largely been replaced by actinolite and dark sub-microscopic material. **e)** Plane-polarized light image of volcanic breccia (DMI17-8-5), showing possible flow foliation in the laminae of dark sub-microscopic material. Volcanic clasts are aphanitic to plagioclase porphyritic and composed of chlorite+actinolite±plagioclase. **f)** Polished slab of volcanic breccia (DMI17-1-10), showing well-developed laminae within a breccia fragment, interpreted as relict flow foliation.

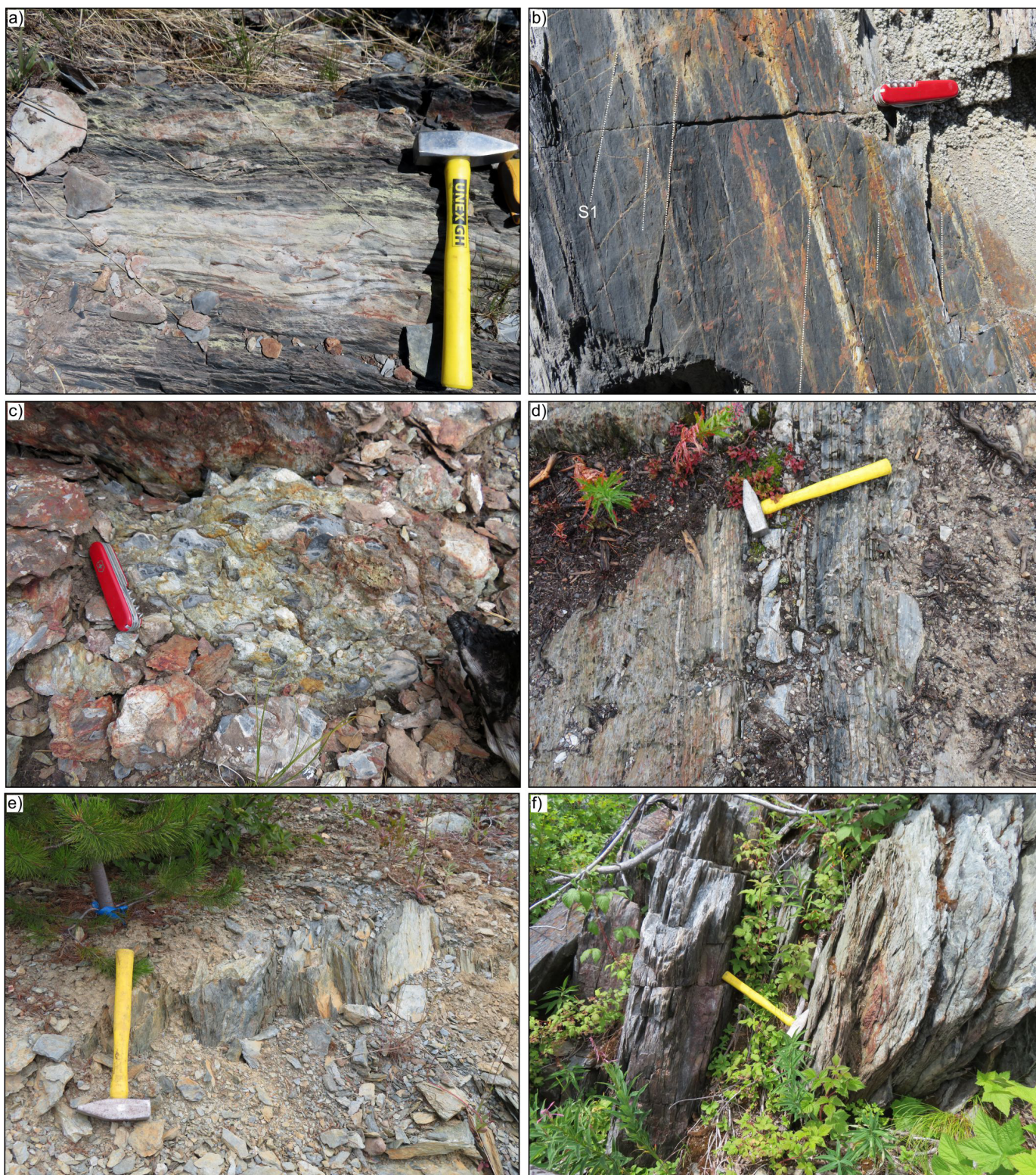


Fig. 8. **a)** Dark, schistose meta-argillite of the Sitlika assemblage, interbedded with light-weathering, weakly-schistose, fine-grained sandstone. Local, discontinuous lamination is evident in the sandstone. Schistosity and bedding are parallel. **b)** Finely bedded meta-argillite of the Sitlika assemblage. Bedding and cleavage have steep, but opposing senses of dip. **c)** Monomictic limestone-cobble conglomerate of the Sitlika assemblage, with a medium- to coarse-grained, lithic-rich, sandstone matrix. Limestone clasts are rounded and typically oblate, and locally contain echinoderm macrofossils. Cleavage is well developed and steeply dipping. **d)** Argillaceous chert of the Sowchea succession with well-developed, bedding-parallel, steeply dipping cleavage. Bedding thickness decreases and argillaceous content increases to the left side of the photograph. **e)** Phyllitic schist of the Sowchea succession with steeply dipping cleavage. **f)** Interbedded dark-grey chert and highly-fissile pyritiferous phyllite of the Rubyrock igneous complex west of the Baptiste deposit.

of the Rubyrock igneous complex, west of the Trembleur ultramafite near the Baptiste deposit (Fig. 2). The local presence of chert suggests a possible Sowchea succession affinity of these relatively rare metasedimentary rocks. However, this correlation is speculative and masked by complexity induced by voluminous intrusion of mafic magma and the resulting relatively high metamorphic grade (amphibolite-facies).

4.3.2.1. Sitlika assemblage

The Sitlika unit consists of black to rusty-weathering, predominantly argillaceous schists, with lesser lithic-rich wacke, and local conglomerate (Figs. 8a-c). The schists contain thin alternating thin layers of siltstone and mudstone and bear a well-developed cleavage that is subparallel, or at low angle, to bedding (Fig. 8b). Less commonly, argillite is interbedded with fine-grained sandstone, which is itself locally laminated (Fig. 8a). Rusty-weathering conglomerate (Fig. 8c) contains rounded, oblate to discoidal pebbles and cobbles of fossiliferous limestone set in a medium- to coarse-grained lithic sandstone matrix.

4.3.2.2. Sowchea succession

Metasedimentary rocks are a significant component of two belts of rocks we assign to the Sowchea succession (Fig. 2) of Struik et al. (2001; 2007). The metasedimentary rocks are typically siliceous, and range in composition from massive chert, through banded ribbon chert, to finely-bedded cherty argillite (Figs. 8d-e). In the northeastern part of the study area, chert is massive and locally pyritiferous. In the southwestern belt, the fine-grained rocks are predominantly cherty, but are locally argillaceous. Our mapping indicates that, in the eastern part of the study area, metasedimentary rocks of the Sowchea succession may be less extensive than previously considered (cf., Struik et al., 2007) and may be subordinate to mafic metavolcanic rocks. Because rocks in the two belts are similar we reassign the rocks in the southwest that were previously included in the Rubyrock igneous complex (unit PTrCRgs of Struik et al., 2007) to the Sowchea succession.

4.3.2.3. Metasedimentary rocks in the Rubyrock igneous complex

Rusty weathering, grey-green, weakly magnetic phyllite outcrops on the southeast side of a northwest-trending brittle fault that juxtaposes it against highly magnetic, strongly serpentinitized, coarse awaruite-bearing metaperidotite of the Baptiste deposit (Fig. 2). Less than 1 km farther west, thin beds of dark grey chert, pyritiferous phyllite, and argillaceous schist are interlayered with light grey- to green-weathering, veined, chaotic amphibolite-facies metaintrusive and/or metavolcanic rocks, characteristic of the Rubyrock intrusive suite.

5. Structure

Previous mapping in the study area (MacIntyre and Schiarizza, 1999; Schiarizza and MacIntyre 1999; Britten, 2017) recognized a predominant subvertical northwest-

southeast trending fabric; our mapping confirms these observations (Figs. 9a and b). Bedding in both the Sowchea succession and the Sitlika assemblage is generally steep (Fig. 9a), dipping either northeast or southwest. A penetrative cleavage, either paralleling the steeply dipping beds or cutting them at a low angle, is best developed in meta-argillite of the Sitlika assemblage (Fig. 8b). Although less well developed, the orientation of cleavage in cherty metasedimentary rocks of the Sowchea succession is indistinguishable from that in the Sitlika assemblage. Moreover, the cleavage in metavolcanic rocks from both the Sowchea succession and Rubyrock igneous complex is identical in orientation to the cleavage in metasedimentary rocks. Minor folds typically plunge gently to the northwest; less commonly fold axes are steep or plunge to the southeast (Fig. 9b). Late deformation is locally manifested by a second, gently-dipping cleavage. Bedding and cleavage systematics of the metasedimentary rocks in the study area are consistent with NE-SW directed shortening.

A steeply dipping, northwest-striking brittle fabric, including spaced cleavage, thin zones (<30 cm) of fragmented carbonate-altered peridotite in a light grey, very fine-grained matrix (Fig. 9c), and zones of shear containing dm- to m-scale knockers of serpentinite in fine-grained foliated, talc±carbonate-rich matrix (Fig. 9d), is variably developed in the Trembleur ultramafic unit. Moreover, the Baptiste deposit, the largest and best studied prospect on the Decar property (Ronacher et al., 2013; Britten, 2017), is located along a major northwest-trending magnetic discontinuity (Verley, 2011) that juxtaposes coarse awaruite-bearing, fissile serpentinite against phyllitic sedimentary rocks, which are tentatively assigned to the sedimentary facies of the Rubyrock igneous complex. These structures are parallel to the predominant northwest-southeast fabric of the flanking volcanic-sedimentary successions.

6. Summary

The Cache Creek terrane in the Decar area of central British Columbia comprises variably serpentinitized and carbonate-altered mantle tectonite (Trembleur ultramafite), greenschist to amphibolite-facies mafic intrusive rocks and minor fine-grained sedimentary rocks (Rubyrock igneous complex), interlayered aphanitic volcanic flows, volcanic breccias, and cherty sedimentary rocks (Sowchea succession), and predominantly fine-grained siliciclastic sedimentary rocks (Sitlika assemblage). Volcano-sedimentary units are broadly subdivided into the predominantly volcanic, chert-rich Sowchea succession and the argillaceous, volcanic-free (Sitlika assemblage). This subdivision, however, must ultimately be confirmed by the geochemical affinity of volcanic units. A pervasive northwest-southeast trending fabric reflects significant northeast-southwest directed shortening, possibly during the collision between the Cache Creek terrane with Stikinia (Struik et al., 2001; English and Johnston, 2005).

Acknowledgments

We thank FPX Nickel Corp. for discussion and access to

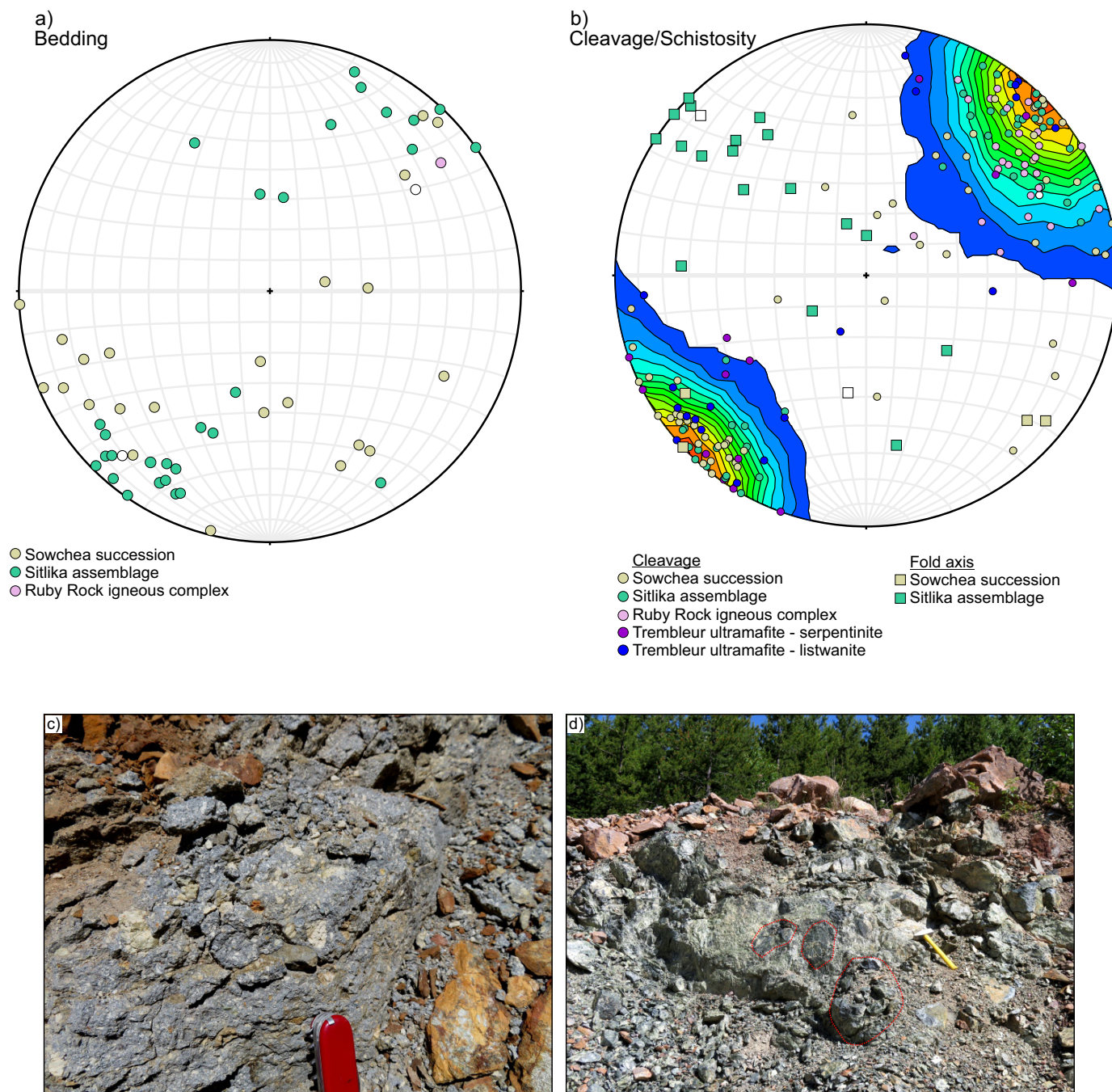


Fig. 9. Equal-area stereonet plots of poles to **a)** bedding and **b)** cleavage (with contours) and minor fold axes. Only the predominant cleavage sets are plotted. Plots and contours were produced using Stereonet 9.5. (Allmendinger et al., 2011; Cardozo and Allmendinger, 2013). **c)** Late, brittle fault in listwanite composed of angular, white weathering carbonate clasts (listwanite) in a very fine-grained, light grey matrix (possible pseudotachylite). **d)** A large (~10 m) block of heterogeneous serpentinite hosted within a zone of strong listwanite alteration. Within the serpentinite, large sub-rounded knockers of massive dark green serpentinite are surrounded by softer, light green, talc-rich matrix.

data. Tl'azt'en Nation and Bev John are thanked for hospitality. Reviews by L. Diakow and L. Aspeler improved the clarity and quality of this paper.

References cited

Ahmed Z., and Bevan J.C., 1981. Awaruite, iridian awaruite, and a new Ru-Os-Ir-Ni-Fe alloy from the Sakhakot-Qila complex, Malakand Agency, Pakistan. *Mineralogical Magazine*, 44, 225-230.

Allmendinger R.W., Cardozo N., and Fisher, D., 2011. *Structural geology algorithms: vectors and tensors*, 1st ed. Cambridge University Press, 302 p.

Beard, J.S., and Hopkinson, L., 2000. A fossil, serpentization-related hydrothermal vent, Ocean Drilling Program Leg 173, Site 1068 (Iberia Abyssal Plain): Some aspects of mineral and fluid chemistry. *Journal of Geophysical Research*, 105, 16,527-16,539.

Boudier, F., and Nicolas, A., 1985. Harzburgite and lherzolite subtypes in ophiolitic and oceanic environments. *Earth and Planetary Science Letters*, 76, 84-92.

- Britten, R., 2017. Regional metallogeny and genesis of a new deposit type-disseminated awaruite (Ni₃Fe) mineralization hosted in the Cache Creek terrane. *Economic Geology*, 112, 517-550.
- Cardozo, N., and Allmendinger, R.W., 2013. Spherical projections with OSX Stereonet. *Computers and Geosciences*, 51, 193-205.
- Chamberlain, J.A., McLeod, C.R., Traill, R.J., and Lachance, G.R., 1965. Native metals in the Muskox Intrusion. *Canadian Journal of Earth Sciences*, 2, 188-215.
- English, J.M., and Johnston, S.T., 2005. Collisional orogenesis in the northern Canadian Cordillera: Implications for Cordilleran crustal structure, ophiolite emplacement, continental growth, and the terrane hypothesis. *Earth and Planetary Science Letters*, 232, 333-344.
- English, J.M., Mihalynuk, M.G., and Johnston, S.T., 2010. Geochemistry of the northern Cache Creek terrane and implications for accretionary processes in the Canadian Cordillera. *Canadian Journal of Earth Sciences*, 47, 13-34.
- Evans, B.W., Hattori, K., and Baronnet, A., 2013. Serpentinite: What, why, where? *Elements*, 9, 99-106.
- Foustoukos, D.I., Bizimis, M., Frisby, C., and Shirey, S.B., 2015. Redox controls on Ni-Fe-PGE mineralization and Re/Os fractionation during serpentinization of abyssal peridotite. *Geochimica et Cosmochimica Acta*, 150, 11-25.
- Frost, B.R., 1985. On the stability of sulfides, oxides, and native metals in serpentinite. *Journal of Petrology*, 26, 31-63.
- Frost, R.B., and Beard, J.S., 2007. On silica activity and serpentinization. *Journal of Petrology*, 48, 1351-1368.
- Hansen, L.D., Dipple, G.M., Gordon, T.M., and Kellett, D.A., 2005. Carbonated serpentinite (Listwanite) at Atlin, British Columbia: a geological analogue to carbon dioxide sequestration. *Canadian Mineralogist*, 43, 225-239.
- Kelemen, P.B., and Dick, H.J.B., 1995. Focused melt flow and localized deformation in the upper mantle: juxtaposition of replacive dunite and ductile shear zones in the Josephine peridotite, SW Oregon. *Journal of Geophysical Research*, 100, 423-438.
- Klein, F., and Bach, W., 2009. Fe-Ni-Co-O-S phase relations in peridotite-seawater interactions. *Journal of Petrology*, 50, 37-59.
- Lapierre, H., Bosch, D., Tardy, M., and Struik, L.C., 2003. Late Paleozoic and Triassic plume-derived magmas in the Canadian Cordillera played a key role in continental crust growth. *Chemical Geology*, 201, 55-89.
- MacIntyre, D.M., and Schiarizza, P., 1999. Bedrock geology, Cunningham Lake (93K/11, 12, 13, 14). British Columbia Ministry of Energy and Mines, British Columbia Geological Survey Open File 1999-11; scale 1:100,000.
- McGoldrick, S., Zagorevski, A., Canil D., Corriveau, A.-S., Bichlmaier, S., and Carroll, S., 2016. Geology of the Cache Creek Terrane in the Peridotite Peak-Menatatlina Range Area, Northwestern British Columbia (Parts of NTS 104K/15, 16). In: *Geoscience BC Summary of Activities 2015, Report 2016-1*, pp. 149-162.
- McGoldrick, S., Zagorevski, A., and Canil, D., 2017. Geochemistry of volcanic and plutonic rocks from the Nahlin ophiolite with implications for a Permo-Triassic arc in the Cache Creek terrane, northwestern British Columbia. *Canadian Journal of Earth Sciences*, 54, 1214-1227.
- Mercier, J.C.C., and Nicolas, A., 1975. Textures and fabrics of upper-mantle peridotites as illustrated by xenoliths from basalts. *Journal of Petrology*, 16, 454-487.
- Mihalynuk, M.G., Erdmer, P., Ghent, E.D., Cordey, F., Archibald, D.A., Friedman, R.M., and Johannson, G.G., 2004. Coherent French Range blueschist: Subduction to exhumation in less than 2.5 m.y.? *Geological Society of America Bulletin*, 116, 910-922.
- Mihalynuk, M.G., Mountjoy, K.J., Smith M.T., Currie, L.D., Gabites, J.E., Tipper, H.W., Orchard, M.J., Poulton, T.P., and Cordey, F., 1999. Geology and mineral resources of the Tagish Lake area (NTS 104M/ 8, 9, 10E, 15 and 104N/12W), northwestern British Columbia. British Columbia Ministry of Energy and Mines, British Columbia Geological Survey Bulletin 105, 217 p.
- Mihalynuk, M.G., Nelson, J.L., and Diakow, L.J., 1994. Cache Creek terrane entrapment: Oroclinal paradox within the Canadian Cordillera. *Tectonics*, 13, 575-595.
- Monger, J.W.H., 1975. Upper Paleozoic rocks of the Atlin terrane, northwestern British Columbia and south-central Yukon. Geological Survey of Canada, Paper 74-47, 63 p.
- Monger, J.W.H., 1977. Upper Paleozoic rocks of the western Canadian Cordillera and their bearing on Cordilleran evolution. *Canadian Journal of Earth Sciences*, 14, 1832-1859.
- Monger, J.W.H., and Ross, C.A., 1971. Distribution of fusulinaceans in the western Canadian Cordillera. *Canadian Journal of Earth Sciences*, 8, 259-278.
- Nelson, J.L., Colpron, M., and Israel, S., 2013. The Cordillera of British Columbia, Yukon, and Alaska: Tectonics and metallogeny. In: Colpron, M., Bissing, T., Rusk, B.G., and Thompson, J.F.H., (Eds.), *Tectonics, Metallogeny, and Discovery: The North American Cordillera and similar accretionary settings*. Society of Economic Geologists, Special Publication 17, pp. 53-109.
- Nickel, E.H., 1956. The occurrence of native nickel-iron in the serpentine rock of the Eastern Townships of the Quebec Province. *Canadian Journal of Earth Sciences*, 6, 307-319.
- Orchard, M.J., Cordey, F., Rui, L., Bamber, E.W., Mamet, B., Struik, L.C., Sano, H., and Taylor, H.J., 2001. Biostratigraphic and biogeographic constraints on the Carboniferous to Jurassic Cache Creek terrane in central British Columbia. *Canadian Journal of Earth Sciences*, 38, 551-578.
- Pearce, J.A., 2008. Geochemical fingerprinting of oceanic basalts with applications to ophiolite classification and the search for Archean oceanic crust. *Lithos*, 100, 14-48.
- Ronacher, E., Baker, J., Palich, J., Broad, P., and Thesen, C., 2013. Resource update-Decar nickel property. Independent technical report, 159 p.
- Schiarizza, P., and MacIntyre, D.G., 1999. Geology of the Babine Lake-Takla Lake area, central British Columbia (93K/11, 12, 13, 14; 93N/3, 4, 5, 6). In: *Geological Fieldwork 1998*, British Columbia Ministry of Energy and Mines, British Columbia Geological Survey Paper 1999-1, pp. 33-68.
- Sciortino, M., Mungall, J.E., and Muinonen, J., 2015. Generation of high-Ni sulfide and alloy phases during serpentinization of dunite in the Dumont sill, Quebec. *Economic Geology*, 110, 733-761.
- Sleep, N.H., Meibom, A., Fridriksson Th., Coleman, R.G., and Bird, D.K., 2004. H₂-rich fluids from serpentinization: Geochemical and biotic implications. *Proceedings of the National Academy of Sciences*, 101, 12,818-12,823.
- Struik, L., Schiarizza, P., Orchard, M., Cordey, F., Sano, H., MacIntyre, D.G., Lapierre, H., and Tardy, M., 2001. Imbricate architecture of the upper Paleozoic to Jurassic oceanic Cache Creek terrane, central British Columbia. *Canadian Journal of Earth Sciences*, 38, 495-514.
- Struik, L.C., MacIntyre, D.G., and Williams, S.P., 2007. Nechako NATMAP project: A digital suite of geoscience information for central British Columbia. Geological Survey of Canada Open File 5623.
- Tardy, M., Lapierre, H., Struik, L.C., Bosch, D., and Brunet, P., 2001. The influence of mantle plume in the genesis of the Cache Creek oceanic igneous rocks: implications for the geodynamic evolution of the inner accreted terranes of the Canadian Cordillera. *Canadian Journal of Earth Sciences*, 38, 515-534.
- Verley, C.G., 2011. Report on the Decar Nickel property. Assessment Report, 52 p. Downloaded from SEDAR, (<https://www.sedar.com/DisplayCompanyDocuments.do?lang=EN&issuerNo=00004553>).